JOURNAL OF QUATERNARY SCIENCE (2023) 1–10 ISSN 0267-8179. DOI: 10.1002/jqs.3519

JQS Journal of Quaternary Science QRA Quaternary Research Association

Developing a South Pacific tephra framework: Initial results from a Samoan Holocene sequence

ANNA J. BOURNE,[1,2]* **DAVID A. SEAR,**[2] **PETE G. LANGDON**[2] **and SHANE J. CRONIN**[3]
[1]School of Geography, Queen Mary University of London, London, UK
[2]School of Geography and Environmental Science, University of Southampton, Highfield, Southampton, UK
[3]School of Environment, University of Auckland, New Zealand

Received 18 July 2022; Revised 28 February 2023; Accepted 12 March 2023

ABSTRACT: Tephra preserved in sediments form useful isochronous marker layers, linking disparate geological, palaeoenvironmental and archaeological records. The application of tephrochronology is greatly enhanced through the detection of macroscopically invisible tephra (cryptotephra). Here, we identify two discrete cryptotephra in Samoan lake sediments, the first identification of cryptotephra in the region outside of New Zealand. Geochemical data suggest one ash layer is from a local Samoan source, providing the first data on an eruption of this age, adding to knowledge of the local volcanic record. The second has a distinctive rhyolitic glass composition, which matches either that of Raoul Island in the Kermadec Arc (1800 km south of Samoa), or two currently submarine volcanoes in the Tongan Arc, 'Volcano F' and Lateiki/Metis Shoal (550 and 700 km south of Samoa, respectively). In all possible source cases, this points to a regionally significant eruption of a Kermadec–Tongan volcano at ca. 10 000 a BP. The study marks the first step in the establishment of a South Pacific tephra framework that can be used to answer questions about the synchronicity of changes in hydroclimate, vegetation and early Polynesian migration patterns, as well as providing more information on the volcanic history of Pacific island volcanoes.

KEYWORDS: Holocene; Kermadec–Tongan volcano; Samoa; South Pacific; tephra

Introduction

The recent eruption of the Hunga Tonga-Hunga Ha'apai volcano on 15 January 2022 demonstrates the impacts that large explosive volcanic eruptions can have on the South Pacific islands but also further afield. Ashfall and the associated tsunami damaged all the islands of Tonga with the entire Pacific Rim being placed on tsunami watch (Zuo et al., 2022). The eruption has also caused scientists to begin to re-evaluate the hazards posed by submarine volcanoes, which are often poorly monitored (Poli & Shapiro, 2022; Witze, 2022).

In addition to being volcanically active, the South Pacific Ocean plays an important part in the global climate system (Brown et al., 2020) and the archipelagos of Polynesia in the South Pacific are believed to be the last habitable places on Earth colonized by humans (Sear et al., 2020). The late colonization of many Pacific islands makes them ideal locations to study natural environments prior to the arrival of humans and their subsequent impact. However, to understand the effect of colonization, there is an urgent need to determine the background context of the late Holocene climate variation in this region. In the tropical South Pacific, this requires a detailed reconstruction of the South Pacific Convergence Zone (SPCZ) over centennial to multi-millennial timescales (Brown et al., 2020). The SPCZ may have influenced human behaviour and migration routes (Anderson et al., 2006). New work is attempting to refine this, using lake sediment archives, hydroclimate reconstructions from algal lipid and leaf wax biomarkers, and carefully constructed chronologies (Sear et al., 2020). While lake sediments preserve evidence of these competing influences (e.g. Gosling et al., 2020), to date there is a paucity of Holocene palaeoclimatic data for this region. In the Eastern and Southern Pacific only a few islands have been studied in detail, and researchers have demonstrated that they contain high-resolution environmental records, notably in the Galápagos (Conroy et al., 2008), Rapa Nui (Roman et al., 2021; Saez et al., 2009) the Cook Islands (Hassall, 2017), 'Uvea (Wallis and Futuna: Maloney et al., 2022), Samoa (Gosling et al., 2020; Hassall, 2017) and Vanuatu (Sear et al., 2020). However, constructing chronologies to link sediment records from widely separated islands remains challenging. Dating individual records from islands relies on often limited radiocarbon dating, and the inability to synchronize and compare records precisely compromises a full appraisal of the interactions between palaeoenvironmental, palaeoclimate and archaeological research.

Tephrochronology has the potential to overcome some of the problems of synchronizing sedimentary and vegetation records from South Pacific islands, as well as providing insights into the volcanic history of the region. Volcanic ash (tephra) is rapidly dispersed and deposited over wide areas following an explosive eruption and can be correlated to eruptions based on their chemical composition (Lowe, 2011). Such tephra layers provide isochronous marker horizons that can be used to connect disparate archives and, where independent age estimates for an eruption exist, to contribute additional chronological information (e.g. Bourne et al., 2015). This approach has been greatly enhanced through the detection of macroscopically invisible volcanic glass particles (cryptotephra), which can extend the

---

*Correspondence: Anna J. Bourne, as above.
Email: a.bourne@qmul.ac.uk

application of tephrochronology up to thousands of kilometres from source volcanoes (Davies, 2015). Cryptotephras have resolved questions regarding the timing and dispersal of early Humans in Europe and the North Atlantic region (Lowe et al., 2015), and the potential exists to apply a similar approach in the volcanically active South Pacific region, where the presence of cryptotephras may be particularly useful as chronological controls beyond the limit of radiocarbon as the region lacks other suitable materials for dating in this time period.

The South Pacific has been volcanically active throughout the Quaternary, with many volcanic eruptions originating from a range of geochemically distinct sources (Cole-Dai et al., 1997). However, with the exception of New Zealand (Hopkins et al., 2021) relatively little is known about tephra layers from other South Pacific volcanoes throughout the Holocene (the time period of interest in this study) (Fig. 1). Table 1 summarizes the available published information about tephra layers in the region. This study presents the first step in the development of a Holocene South Pacific tephra framework with a tephrochronological record from Lake Lanoto'o, Upolu, Samoa.

Regional setting

The Samoan archipelago

The Samoan archipelago lies within the central Pacific Ocean (13–14°S, 170–173°W), with two main islands, Savai'i and Upolu, making up 96% of the landmass (total 2934 km^2; Fig. 1). Samoa lies at the northern termination of the subduction volcanism of the Tongan Arc, but it contrasts by erupting ocean island basalt magmas, more akin to Hawaiian-type volcanism (Hart et al., 2004; Hawkins, 1976; Kear, 1967; Kear & Wood, 1959). The islands are remnant basaltic shields that were heavily eroded during the Pliocene and early Pleistocene, and are now buried by late Pleistocene lava flow deposits and scoria cones (Stearns, 1944). The last known volcanic eruptions in Samoa were in AD 1760, 1902 and 1905–1911 on Savai'i (Anderson, 1912; Németh & Cronin, 2009; Venzke, 2013).

The climate of Samoa is principally controlled by the SPCZ and its interplay with the Trade Winds (Fig. 1). The most noticeable effect of the SPCZ and its location is on precipitation, which varies from >400 mm (January) to <150 mm (July) (Hassall, 2017). Precipitation characterizes seasonality in Samoa, as temperatures are relatively constant throughout the year (mean monthly minimum 23–24 °C and maximum 29–30 °C (Gosling et al., 2020).

Upolu Island has a tropical climate, with a mean annual temperature of 26.6 °C and mean annual precipitation of ~2800 mm (Lagomauitumua, 2011); the southern, more windward side of the island receives slightly more rain due to the location of the southeast trade wind belt. Whilst the island has no distinct dry season, November and April are slightly warmer and wetter with increased frequency of tropical cyclones (Mueller-Dombois & Fosberg, 1998). Different El Niño Southern Oscillation (ENSO) phases lead to strong year-to-year climatic variation due to movement of the SPCZ; the El Niño phase leads to drier conditions and the La Niña phase delivers greater wet season rainfall (Lagomauitumua, 2011). Sedimentary archives of past climate on Samoa have been reconstructed over the Holocene and show abrupt changes in precipitation proxies interpreted to indicate regional changes in the position and intensity of the SPCZ (Hassall, 2017).

Samoan volcanism

There has been active volcanism in Samoa from the Pliocene to present times (Kear & Wood, 1959; Natland, 1980). Shield growth in Savai'i is inferred to have been between 5.29 and 2 Ma, starting with ocean island basalt and terminating with evolved, trachytic lavas (Koppers et al., 2008). Rejuvenated volcanism followed the shield stage from ~386 ka, including several sites of activity in the last 2000 years, and erupting as recently as 1905–1911 (Fepuleai, 2016; Németh & Cronin, 2009; Workman et al., 2004).

Kear and Wood (1959) mapped (Western) Samoa lavas into six formations named after villages and districts where these lavas are well exposed. From the oldest to the youngest formation, they are the Fagaloa Volcanic Formation (Pliocene to Middle Pleistocene), Salani Volcanic Formation (Middle to Late Pleistocene), Mulifanua Volcanic Formation (Late Pleistocene), Lefaga Volcanic Formation (Early Holocene), Puapua Volcanic Formation (Middle to Late Holocene) and Aopo Volcanic Formation (Historical) (Fig. 2a). Subsequently, with additional radiocarbon ages and mapping, Nemeth and Cronin (2009) and Fepuleai (2016) noted that these formations are time-transgressive. Fepuleai (2016) suggested that three formations represent active volcanism during human occupation in Samoa, including the Aopo Formation in northern Savai'I, Lefaga Formation in southwest Upolu, as well as the Puapua and Mulifanua Formations in cones within broad rift zones across Samoa's main islands (Fig. 2). Upolu cones are aligned along a central rift along the long-axis of the island.

Volcanism coeval with human occupation is characterized by low-volume scoria and spatter cone building along with lava flows over weeks to several years of total eruptive time (Németh & Cronin, 2009). The majority of these eruptions exhibit mainly Hawaiian-style fire fountaining activity with associated eruption columns probably less than a few kilometres in height (Németh & Cronin, 2009). There is very little radiometric dating of volcanism on Samoa. Many morphologically young scoria cones occur, but systematic morphometric study of the Samoan cones similar to those elsewhere (Kereszturi & Németh, 2012) has not yet been performed.

Material and Methods

Study site

Lake Lanoto'o (171°50′W, 13°54′S) is a 0.11-km^2 volcanic crater lake at the centre of Upolu island ~760 m above sea level (asl) with a catchment area of 0.23 km^2. Today the lake is ~400 m wide with a maximum depth of 17.5 m (Fig. 1); in the surface layers lake water is pH 7, with a temperature of ~27 °C, oxygen saturation of 105% and a conductivity of 15 $\mu s\ cm^{-1}$ (measured in September 2014). At ~10 m depth a thermocline results in a relatively abrupt change to cooler (23 °C) anoxic conditions (dissolved oxygen 10%), pH 4, and increased conductivity (21 $\mu s\ cm^{-1}$) (Gosling et al., 2020; Hassall, 2017).

Sediment recovery

A sequence of overlapping cores was obtained from the deepest region of Lake Lanoto'o in September 2014 (Fig. 1 and Gosling et al., 2020). A UWITEC gravity-type corer was used

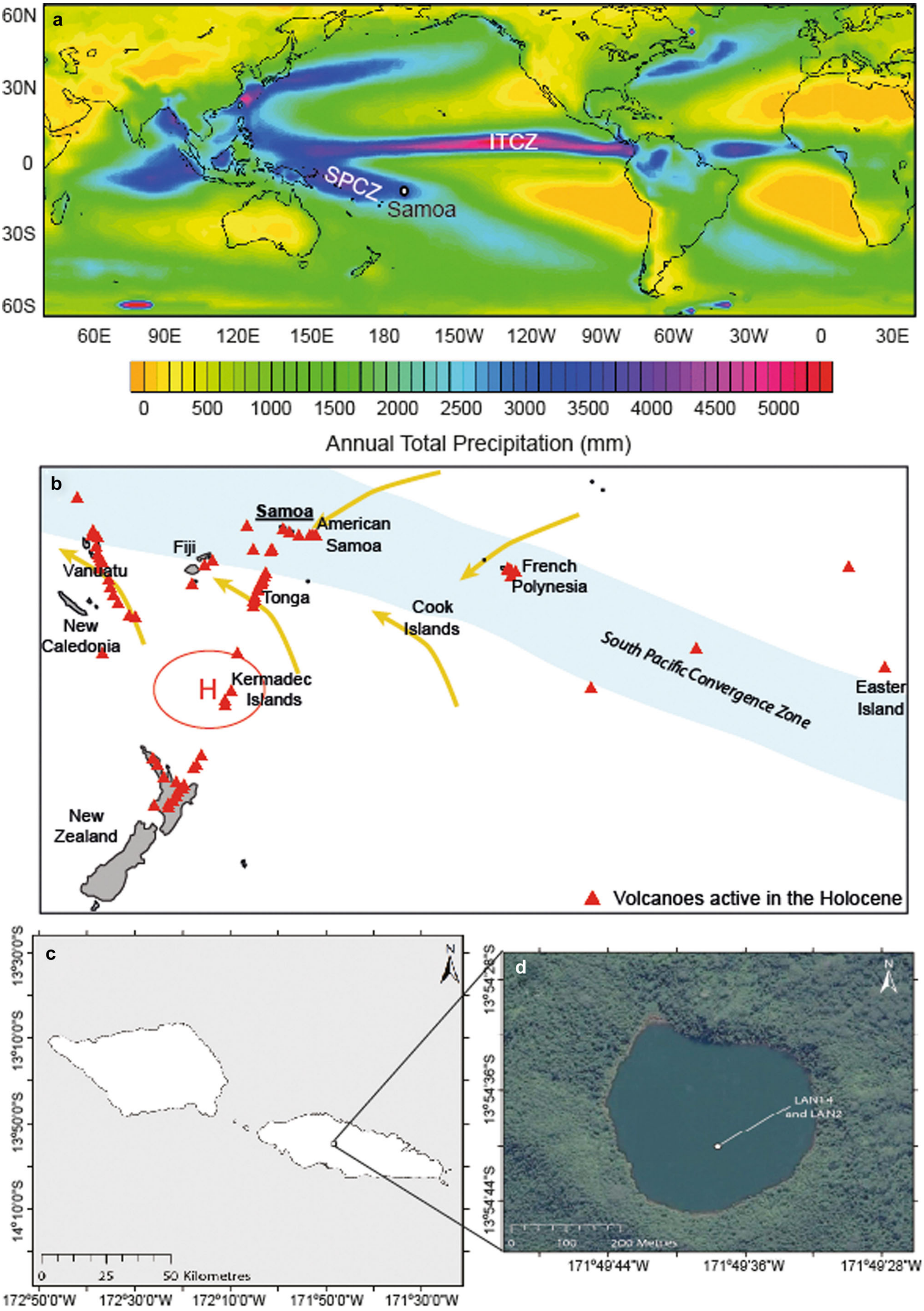

Figure 1. Location map. (a) Samoa lies in the South Pacific Convergence Zone (SPCZ) with a climate strongly influenced by El Niño Southern Oscillation (ENSO). (b) Location of volcanoes that have been active in the Holocene. (c) Map of Samoa; the square box indicates the location of Lake Lanoto'o on Upolu island. (d) Lake Lanoto'o with the coring location of LAN14 marked. Adapted from Hassell (2017). [Color figure can be viewed at wileyonlinelibrary.com]

Table 1. Database of tephra layers described within sediments from Fiji, the Kermadec islands, New Zealand, Samoa, Tonga and Vanuatu volcanic sources.

Tephra name	Alternative name(s)	Caldera source	Age	Geochemical data	Reference(s)
Fiji					
De Voeux tephra		Taveuni	1290–1410 AD	N	Cronin 2000
Tavuyaga tephra		Taveuni	1260–1390 AD	N	Cronin 2000
Vana Kei Vuna tephra		Taveuni	1020–1290 AD	N	Cronin 2000
Soqulu tephra		Taveuni	600–670 AD	N	Cronin 2000
De Voeux 1 tephra		Taveuni	340–450 AD	N	Cronin 2000
Likuvausimi tephra		Taveuni	230–400 AD	N	Cronin 2000
Ura tephra		Taveuni	400–250 BC	N	Cronin 2000
Nadawa tephra		Taveuni	4900–3370 BC	N	Cronin 2000
Kermadec Islands					
Sandy Bay Tuff		Macauley Island	7571–6754 cal a BP	Y	Shane and Wright 2011
1/87		Macauley Island?	5600 cal a BP	Y	Shane and Wright 2011
1/165		Macauley Island?	8400 cal a BP	Y	Shane and Wright 2011
Sentinel tephra		Denham Bay Caldera?	ca. 1650 to 1800 AD	N	Worthington et al., 1999; Latter et al., 1992
Rangitahua		Raoul Caldera	ca. 1600 to 1680 AD	N	Worthington et al., 1999; Latter et al., 1992
Expedition Crater		Raoul Caldera	1100 cal a BP	N	Worthington et al., 1999; Latter et al., 1992
Green Lake Pumice		Raoul Caldera	1400 cal a BP	N	Worthington et al., 1999; Latter et al., 1992
Rayner Tephra		Raoul Caldera	1550 cal a BP	N	Worthington et al., 1999; Latter et al., 1992
Judith Tephra		Denham Bay Caldera?	1850 cal a BP	N	Worthington et al., 1999; Latter et al., 1992
Bell Tephra		Denham Bay Caldera?	2050 cal a BP	N	Worthington et al., 1999; Latter et al., 1992
Fleetwood Tephra		Denham Bay Caldera	2200 cal a BP	Y	Worthington et al., 1999; Latter et al., 1992
Oneraki Tephra		Raoul Caldera	3150 cal a BP	N	Worthington et al., 1999; Latter et al., 1992
Matatirohia Tephra		Raoul Caldera	3700 cal a BP	N	Worthington et al., 1999; Latter et al., 1992
10/19		Raoul Island?	<10 000 cal a BP	Y	Shane and Wright 2011
7/6		Raoul Island?	<10 000 cal a BP	Y	Shane and Wright 2011
1/97		Raoul Island?	6000 cal a BP	Y	Shane and Wright 2011
1/140		Raoul Island?	8000 cal a BP	Y	Shane and Wright 2011
4/18		Raoul Island?	<9700 cal a BP	Y	Shane and Wright 2011
New Zealand					
Tarawera		Tarawera	1886 AD	Y	Hopkins et al., 2021*
Kaharoa		Okataina	636 ± 12 cal a BP	Y	Hopkins et al., 2021*
Taupō	Unit Y	Taupō	1718 ± 10 cal a BP	Y	Hopkins et al., 2021*
Mapara	Unit X	Taupō	2059 ± 118 cal a BP	Y	Hopkins et al., 2021*
Whakaipo	Unit V	Taupō	2800 ± 60 cal a BP	Y	Hopkins et al., 2021*
Waimihia	Unit S	Taupō	3382 ± 50 cal a BP	Y	Hopkins et al., 2021*
Stent	Unit Q	Taupō	4322 ± 112 cal a BP	Y	Hopkins et al., 2021*
Unit K (Taupō series)		Taupō	5088 ± 73 cal a BP	Y	Hopkins et al., 2021*
Whakatāne		Okataina	5542 ± 48 cal a BP	Y	Hopkins et al., 2021*
Tuhua		Mayor Island	7637 ± 100 cal a BP	Y	Hopkins et al., 2021*
Mamaku		Okataina	7992 ± 58 cal a BP	Y	Hopkins et al., 2021*
Rotoma		Okataina	9472 ± 40 cal a BP	Y	Hopkins et al., 2021*
Ōpepe	Unit E	Taupō	10004 ± 122 cal a BP	Y	Hopkins et al., 2021*
Samoa					
Tephra bed-1		Unknown	3400 cal a BP	N	Fepuleai 2016
Tonga					
Fonualei		Fonualei	1846 AD	Y	Turner et al., 2012
Niuafo'ou		Niuafo'ou	1886 AD	Y	Regelous et al., 2008
Vanuatu					
Kuwae 1452		Kuwae	1452 AD	Y	Gao et al., 2006; Witter and Self, 2007
EMO 128.5 cm		Kuwae	1452 AD	N	Sear et al., 2020
Level 142-143		Unknown	1400 cal a BP	N	Wirrmann et al., 2011
Level 277-282 cm		Unknown	2100–2090 cal a BP	N	Wirrmann et al., 2011
Level 292 cm		Unknown	c.2165 cal a BP	N	Wirrmann et al., 2011
Ambrym		Ambrym	1913 AD	Y	Németh and Cronin, 2011
Yasur (various)		Yasur		Y	Firth et al., 2014

*And references therein.

to recover the upper 60 cm. A Geocore cam-modified piston corer was used to retrieve overlapping sediment cores to a depth of 262 cm below the mud–water interface, below which point the sediments were impenetrable with this coring system. All cores were stored intact in airtight tubes and kept in cold storage (+4 °C) at the University of Southampton. Sub-samples were subsequently extracted from the cores for radiocarbon dating and tephra analysis.

Age vs. depth model

Radionuclide dating was used to generate an age model for the Lake Lanoto'o sediments by Gosling et al. (2020). A combination of ^{137}Cs and ^{210}Pb measurements from the surface core and 17 radiocarbon (^{14}C) measurements from bulk (13) and organic plant material (four) samples were used to create an age vs. depth model for Lake Lanoto'o in BACON 2.2 Bayesian modelling software (Blaauw & Christen, 2011). BACON highlighted two samples (LAN14-2-2 11–12 cm and LAN14-1-3 17–18 cm) that are outliers, the former being older than expected and the latter being younger than expected; the remainder of the dates are stratigraphically consistent throughout the sequence. Re-analysis of the core correlation since Gosling et al. (2020) has resulted in a revised updated age–depth model that we present in this paper. The result is a relatively small reduction in master core length compared with the Gosling et al. model. The revised age–depth model for the Lake Lanoto'o core is given in the Supporting Information, and for the last 2000 years in Maloney et al. (2022).

Tephrochronological methods

Tephra extraction

Contiguous 5-cm-long sub-samples were extracted from throughout the entire core sequence and sieved to recover all sediment particles between 80 and 15 μm in size. The sieve mesh was changed regularly to avoid cross-contamination. This fraction was then immersed in sodium polytungstate of prepared density using a cleaning float of 2.00 g cm^{-3} and an extraction float of 2.55 g cm^{-3} (Blockley et al., 2005). The supernatant of the extraction float was mounted on glass slides in Canada Balsam and scanned for the presence of glass shards under an optical microscope fitted with cross-polarising filters. In addition, the >2.55 g cm^{-3} residue was also mounted on glass slides to check for the presence of basaltic glass particles. The numbers of shards were then counted and concentrations per gram of sample (dry weight) calculated. Where tephra shards were identified the sample resolution was refined to 1 cm.

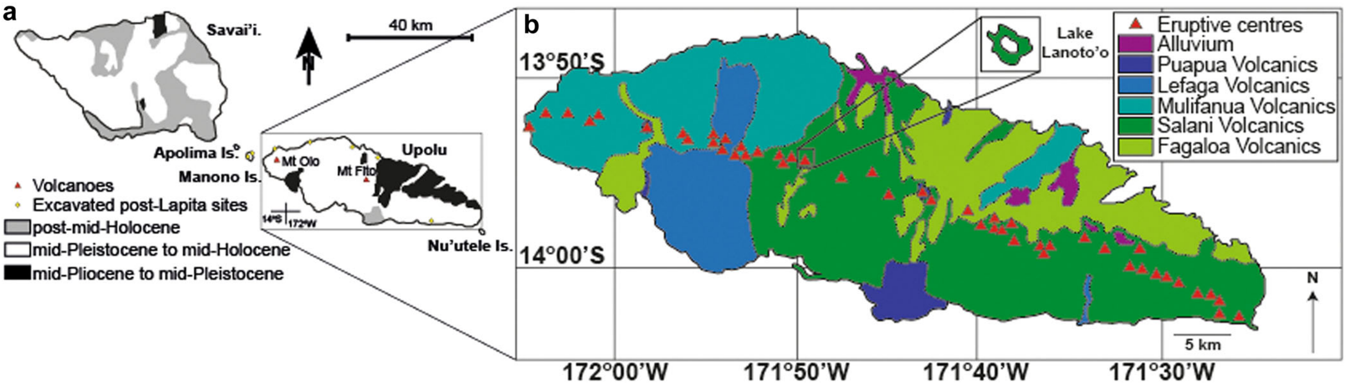

Figure 2. (a) Surface distribution of volcanic stratigraphy units of Western Samoa (redrawn from Nemeth and Cronin 2009). (b) Geological map of Upolu showing the six volcanic units and eruptive centres (redrawn from Kear & Wood, 1959). [Color figure can be viewed at wileyonlinelibrary.com]

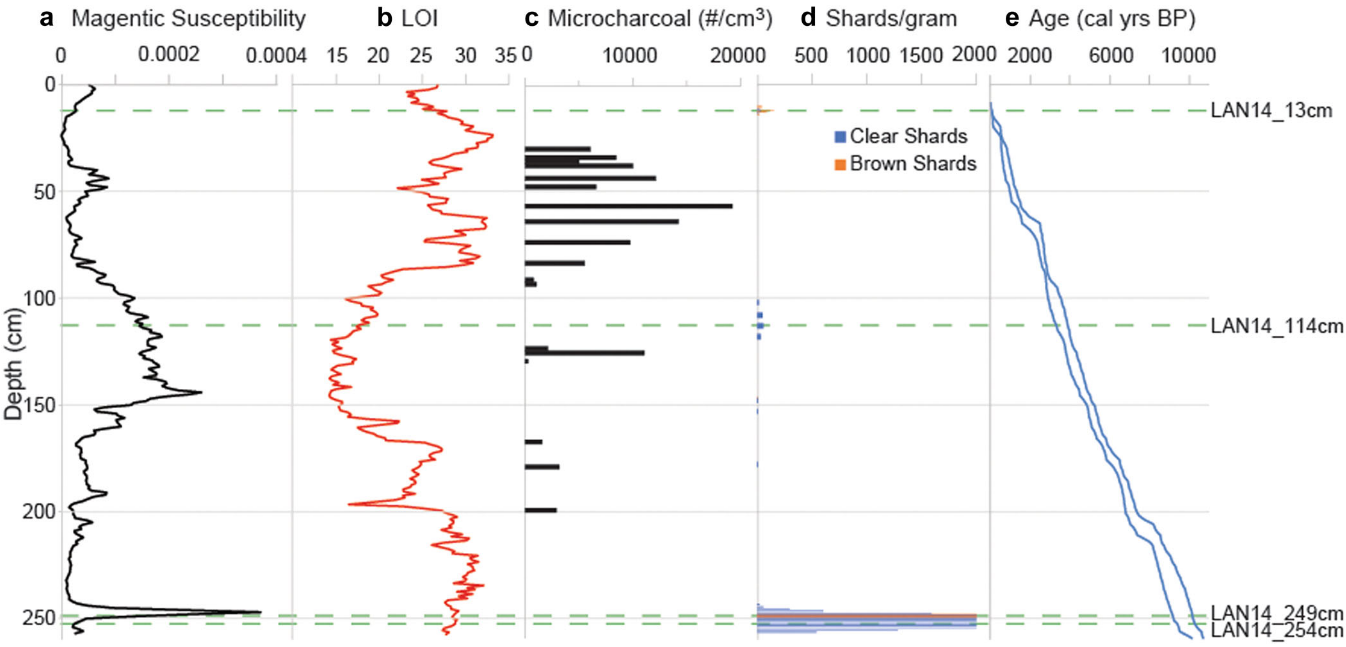

Figure 3. Lake Lanoto'o magnetic susceptibility, loss on ignition, microcharcoal particles (from Gosling et al., 2020), tephra shard counts and age–depth model showing 2-sigma error bands. [Color figure can be viewed at wileyonlinelibrary.com]

Labelling of tephra layers

Individual discrete tephra layers were assigned a unique code; this refers to the composite depth in the profile at which the peak glass shard concentration was detected in the sequence.

Geochemical analysis of glass shards

In tephra layers selected for geochemical analysis, glass shards extracted from the layers were mounted in Steurs Epofix epoxy resin. Mounts were sectioned and polished and examined using reflected light microscopy. Chemical analysis of vitreous material was undertaken using wavelength-dispersive spectrometry electron probe microanalysis (WDS-EPMA). Analysis was carried using a Cameca SX100 microprobe housed at the Department of Geosciences, University of Edinburgh. This operated using a defocused 5-μm beam size, a 15-kV voltage and a 2-nA current (for Na, K, Si, Al, Mg, Fe and Ca) or an 80-nA current (for F, Cl, S, Mn, Ti and P) (Hayward, 2012). The machine was calibrated using modified standard blocks supplied by the instrument manufacturers while a combination of internally assayed Lipari and BCR_2G (Jochum et al., 2005; Jochum & Willbold, 2006) were used as secondary standards.

The data were screened for non-glass material and outlier values and samples with analytical totals <95% were excluded and then remaining data were normalized to 100% (Hunt & Hill, 1993).The geochemical results, including data obtained from standards, are provided in the Supporting Information.

Results

Four cryptotephra layers were identified at 5-cm resolution: LAN14_13cm, LAN14_114cm, LAN14_249cm and LAN14_254cm (Fig. 3). It is clear that despite Lake Lanoto'o being a volcanic crater lake, there is no continuous background of glass shards (e.g. from erosion events on crater walls); instead, discrete cryptotephra layers are identified. In all cases the volcanic glass is fresh and shows no evidence of alteration, as described by Fepuleai (2016) from volcanic lake Lanoto from eastern Upolu (not to be confused with lake Lanoto'o in this study) (Fepuleai et al., 2018).

LAN14_13cm

A cryptotephra layer comprising 70 brown shards per gram was identified at a composite depth of 13 cm; the age model dates it to approximately 1887 AD (52.7–73.3 cal a BP). Geochemical data classify is as a shoshonite trachybasalt with SiO_2 concentrations of 48.03–48.73 wt% and K_2O values of 4.14–4.20 wt% (Fig. 4).

LAN14_114cm

A cryptotephra comprising 55 clear shards per gram was originally identified in the 5-cm-resolution samples at a composite depth of 114 cm (Fig. 3); this equated to six tephra shards present on the slide itself. However, when increasing the sampling resolution to 1 cm, no distinct peak in glass shards could be identified; instead shards were dispersed over the sample, with one or two shards present in a couple of centimetres, and therefore this layer was not subject to further analysis.

LAN14_249cm and LAN14_254cm

Glass shards are present at the base of the core (262 cm) and rise to a significant peak of over 10 000 clear shards per gram at a composite depth of 254 cm; this is coincident with a magnetic susceptibility spike of 0.0004 κ (Kappa) (Fig. 3). These clear shards continue for a further 5 cm but in the 249-cm sample brown shards are also present, warranting classification of LAN14_249cm as a separate layer. Geochemical data from the clear shards in both LAN_249cm and LAN14_254cm are indistinguishable and the layers are classified as tholeiitic rhyolites with SiO_2 concentrations of 71.62–76.29 wt% and K_2O values of 0.75–1.00 wt% (Fig. 4). Unfortunately, geochemical data could not be obtained from the brown shards originally present in the LAN14_249cm sample. These layers are associated with a large magnetic susceptibility spike and the age model dates the LAN14_254cm layer to approximately 9498–10 495 cal a BP.

Discussion

This study demonstrates that discrete cryptotephra layers can be preserved within lake sediments in Samoa. Despite the islands' volcanic origin, there is not a large amount of volcanic material within the lake sediments. This, combined with the fact that the geochemistry of the local volcanic products hinders their direct dating, highlights the potential of using tephrochronology as a stratigraphic and correlation tool in this region.

The geochemistry of the LAN14_13cm layer indicates it is consistent with a local source in the Samoa Volcanic Field (Fig. 4a). The chronology of Holocene volcanic events on Samoa is very poorly resolved. Nemeth and Cronin (2009) provide a radiocarbon age of 230 ± 70 ^{14}C a BP from a lava flow and possible volcanic ash layer in the Lalofasa area on Savai'i island. Calibration of this radiocarbon date gives an age of 1629–1896 AD (Hogg et al., 2020) which is contemporaneous with LAN14_13cm (1887 AD from the age model), but no geochemical data exist to confirm this. There are many broadly contemporaneous eruptions in Tonga (e.g. Niuafo'ou ~450 km away, Tofua ~700 km away and Hunga ~800 km away and several Vanuatu centres >2000 km away) (Venzke, 2013) (Table 1). The limited geochemical data available for these contemporaneous eruptions do not match well with LAN14_13cm (Fig. 5a,b).

Very little information about early Holocene eruptions from South Pacific volcanoes has been published (Crosweller et al., 2012; Venzke, 2013) (Table 1). However, we have ascertained that the composition of the glass in layer LAN14_254cm lies well outside the Samoan Volcanic Field (Fig. 4a), suggesting a more distal Pacific volcanic source. All known radiocarbon-dated tephra sequences in the Tongan arc extend only as far back as ~6500 cal a BP (Cronin et al., 2004; Cronin & Cashman, 2007; Cronin et al., 2008) and compositions of comparatively younger large-scale eruptives from Hunga, Tofua and Fonunelei volcanoes are all more mafic than LAN14_254cm (cf. Brenna et al., 2022; Caulfield et al., 2011; Turner et al., 2012). Other possible sources of large-scale eruptions in the central to northern Tongan arc (500–700 km from the study site) include the submarine calderas of Home Reef, Late'iki (Metis Shoal) and Volcano F (Brandl et al., 2020; Yeo et al., 2022). These have normally only erupted as pumice rafts in recent history, but with lower sea levels at the start of the Holocene they may have produced subaerial tephra. Recent

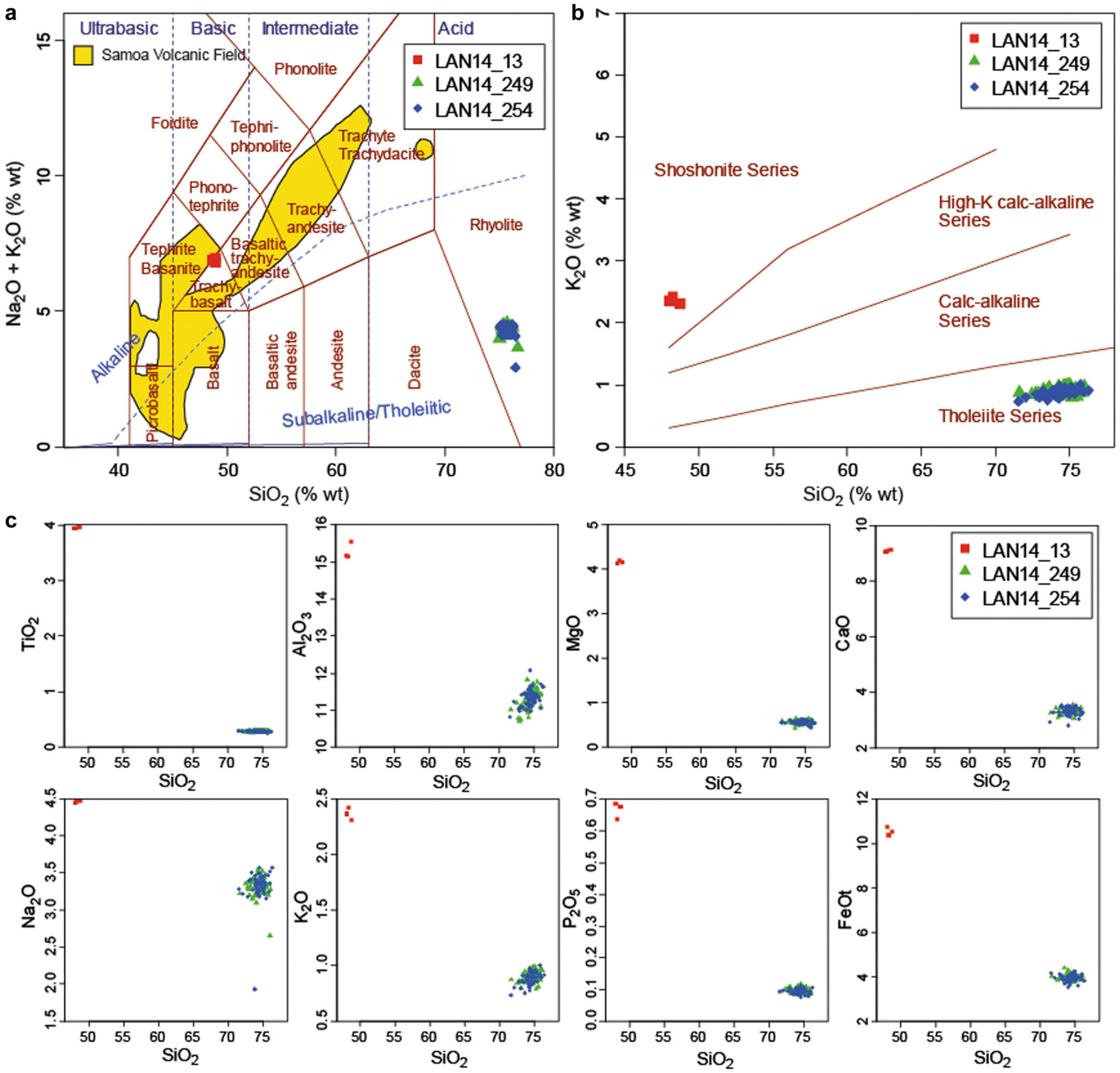

Figure 4. LAN14 geochemical data. (a) Total alkali vs. silica (Le Bas et al., 1986). The Samoa Volcanic Field (yellow) boundary is redrawn from Fepuleai (2016) and Konter and Jackson (2012). (b) SiO_2 vs. K_2O classification and (c) Harker diagrams. [Color figure can be viewed at wileyonlinelibrary.com]

data obtained from sediment samples from these shoals show compositional similarities to LAN14-254cm (Fig. 5c,d).

Further south, at >1300 km from the study site, the Kermadec arc also produces tephra with some compositional affinities to LAN14-254cm. Shane and Wright (2011) identified high-K and low-K Late Quaternary tephras from marine cores around the Kermadec arc, suggesting the low-K rhyolites are probably sourced from Raoul island (1800 km from the site). Two eruptions from New Zealand (~3000 km south) have contemporaneous ages, Rotoma from Okataina (9472 ± 40 cal a BP) and Opepe (Unit E) from the Taupo Volcano (9906 ± 246 cal a BP) (Lowe et al., 2013). However, these tephras are compositionally distinct from LAN14_254cm (Fig. 5c,d) being calc-alkaline rhyolites.

The LAN_254cm data plot within the low-K rhyolite field of the Kermadec arc and similar to some of the historically erupted Late'iki and Volcano F compositions (Fig. 5c,d). Highlighted on Fig. 5c and d are two layers which may be similar in age to LAN14_254cm; the 4/18 has an age <9.7 ka BP and the 10/19 layer is dated to <10 ka BP (Shane and Wright, 2011). While a clear match cannot be made, the more proximal Tongan sources seem the most likely to disperse tephra to Lake Lanoto'o, based on distance, but the Kermadec arc provides a better geochemical match. Whilst a correlation to a specific tephra layer cannot be made, the distinctive composition of this layer means that it could be a useful isochron, if it can be traced in other sequences in the region. It also highlights many unanswered questions about potential distal tephras erupted from Kermadec–Tongan arc volcanoes that are largely small islands or submarine and the implications these eruptions may have had on the environment at the time. Unfortunately the locations of LAN14_13cm and LAN14_254cm lie outside the depths analysed for pollen and charcoal analysis by Gosling et al. (2020) (see Fig. 3) so no comparison of the impact of these potentially large eruptions can be made at this time.

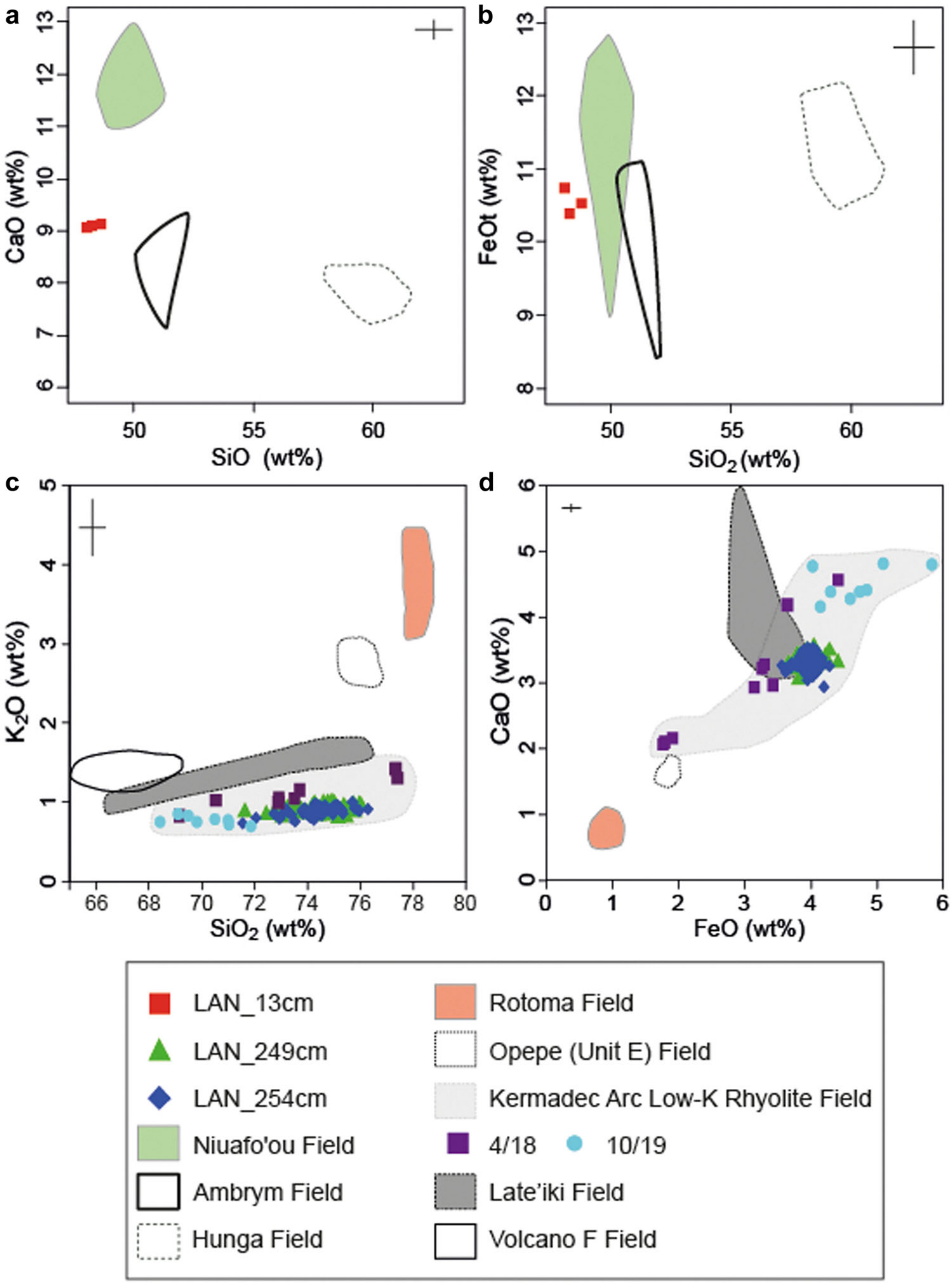

Figure 5. (a, b) LAN14_13cm geochemical data compared to data from contemporaneous eruptions. The Niuafo'ou Field data are from the Lau Basin Lavas (Regelous et al., 2008), the Ambrym Field data are from glass shards of the Hospital-tuff ring of the Ambrym 1913 AD eruption (Németh and Cronin, 2011) and the Hunga Field data are glass data from the Hunga 1100 AD eruption (S. Cronin, pers comm.) and is included in the Supporting Information. (C) LAN14_249cm and LAN14_254cm geochemical data compared to data from contemporaneous eruptions and Tongan geochemical data. The Rotoma field data are from Hopkins et al. (2020) and Smith et al. (2006), the Opepe (Unit E) data are from Hopkins et al. (2020), Lowe et al. (2008) and Smith et al. (2005), and the Kermadec Arc low-K rhyolite, 4/18 and 10/19 data are from Shane and Wright (2011). The Volcano F data are from the 2019 eruption (Brandl et al., 2020) and the Late'iki field data are from the 2019–2020 eruption (Yeo et al., 2022). Two-sigma errors based on the standard data are shown. [Color figure can be viewed at wileyonlinelibrary.com]

The present study also highlights how little is known about the preservation of ash layers in the region outside of New Zealand beyond 2000 years ago (Table 1), therefore demonstrating the potential of further work on cryptotephra layers in this volcanically active region.

Conclusion

This study demonstrates that discrete, far-travelled cryptotephras are preserved in lake records from the volcanically active island of Samoa and highlights the potential for cryptotephra analysis to be expanded in the South Pacific region. Two cryptotephras are dated, described and geochemically characterized. The youngest layer (LAN14_13cm) is indicative of a local Samoan source, suggesting an eruption occurred around 1887 AD. This study shows the potential of adding information to local volcanic histories through the use of cryptotephra layers. The older layer (LAN14_254cm, 9498–10 495 cal a BP) potentially correlates to a source in the Kermadec–Tongan arc. This highlights the potential for identifying tephras from currently submarine volcanoes and whether this represents different volcanic patterns in the past (i.e. with sea-level change) or changes in volcano form with growth and collapse cycles (as observed in Hunga-Tonga-Hunga-Hapa'ai). Whilst neither eruption can be correlated to known eruptions in the region, they form an important first step in developing a South Pacific tephra framework and improving local (e.g. Tongan) volcanic chronologies through the analysis of other sediment cores in the region, work which is currently underway. The study demonstrates the potential for identifying cryptotephra throughout this highly volcanically active region and its value in the identification of large-scale events, which in turn would have had huge implications for palaeoclimate, past vegetation changes as well as influencing human settlement.

Acknowledgements. This work would not have been possible without the guidance, kindness and support of a number of key colleagues from Samoa, including: Taule'ale'ausmai Laavasa Malua and the late Niualuga Evaimalo from the Ministry of Natural Resources and Environment (MNRE) Division of Environment and Conservation, Government of Samoa, who worked with us on providing permissions. We are indebted to Josie Hill, Lucy, Tinifu, Solomano, Ai and Georgia Eves who all provided field assistance. We thank Dr Chris Hayward for his assistance with the use of the electron microprobe at the Tephrochronology Analytical Unit, University of Edinburgh. The Explorers Club Exploration Fund Grant, Gilchrist Expedition Grant and Royal Geographical Society (with the Institute of British Geographers) Monica Cole Grant assisted with travel to Samoa. A special mention to Jon Hassall who originally worked on Lake Lanoto'o for his PhD, funded under an NERC Studentship (to J. Hassall). We acknowledge the support of the NERC Radiocarbon Facility NRCF010001 and specifically dates provided under allocation numbers 2004.0416, 1799.0414 and 1900.0415.

Conflict of Interest Statement—None of the authors have any conflicts of interests to declare.

Data availability statement

The data that supports the findings of this study are available in the supplementary material of this article.

Supporting information

Additional supporting information can be found in the online version of this article.

Abbreviations. ENSO, El Niño Southern Oscillation; ITCZ, Intertropical Convergence Zone; SPCZ, South Pacific Convergence Zone.

References

Anderson, A., Chappell, J., Gagan, M. & Grove, R. (2006) Prehistoric maritime migration in the Pacific islands: an hypothesis of ENSO forcing. *The Holocene*, 16, 1–6.

Anderson, T. (1912) Volcanic craters and explosions. *The Geographical Journal*, 39, 123–129.

Blaauw, M. & Christen, J.A. (2011) Flexible paleoclimate age-depth models using an autoregressive gamma process. *Bayesian Analysis*, 6, 457–474.

Blockley, S.P.E., Pyne-O'Donnell, S.D.F., Lowe, J.J., Matthews, I.P., Stone, A., Pollard, A.M. et al. (2005) A new and less destructive laboratory procedure for the physical separation of distal glass tephra shards from sediments. *Quaternary Science Reviews*, 24, 1952–1960.

Bourne, A.J., Albert, P.G., Matthews, I.P., Trincardi, F., Wulf, S., Asioli, A. et al. (2015) Tephrochronology of core PRAD 1-2 from the Adriatic Sea: insights into Italian explosive volcanism for the period 200–80 ka. *Quaternary Science Reviews*, 116, 28–43.

Brandl, P.A., Schmid, F., Augustin, N., Grevemeyer, I., Arculus, R.J., Devey, C.W. et al. (2020) The 6–8 Aug 2019 eruption of 'Volcano F' in the Tofua Arc, Tonga. *Journal of Volcanology and Geothermal Research*, 390, 106695.

Brenna, M., Cronin, S.J., Smith, I.E.M., Pontesilli, A., Tost, M., Barker, S. et al. (2022) Post-caldera volcanism reveals shallow priming of an intra-ocean arc andesitic caldera: Hunga volcano, Tonga, SW Pacific. *Lithos*, 412–413, 106614.

Brown, J.R., Lengaigne, M., Lintner, B.R., Widlansky, M.J., van der Wiel, K., Dutheil, C. et al. (2020) South Pacific Convergence Zone dynamics, variability and impacts in a changing climate. *Nature Reviews Earth & Environment*, 1, 530–543.

Caulfield, J.T., Cronin, S.J., Turner, S.P. & Cooper, L.B. (2011) Mafic Plinian volcanism and ignimbrite emplacement at Tofua volcano, Tonga. *Bulletin of Volcanology*, 73, 1259–1277.

Cole-Dai, J., Mosley-Thompson, E. & Thompson, L.G. (1997) Annually resolved southern hemisphere volcanic history from two Antarctic ice cores. *Journal of Geophysical Research: Atmospheres*, 102, 16761–16771.

Conroy, J.L., Overpeck, J.T., Cole, J.E., Shanahan, T.M. & Steinitz-Kannan, M. (2008) Holocene changes in eastern tropical Pacific climate inferred from a Galápagos lake sediment record. *Quaternary Science Reviews*, 27, 1166–1180.

Cronin, S., Smith, I., Taylor, P. & Platz, T. (2004) *New evidence for widespread, late Holocene, explosive volcanism along the Tongan arc*. Pucon, Chile: IAVCEI General Assembly.

Cronin, S.J. & Cashman, K. (2007) Volcanic oral traditions in hazard assessment and mitigation. In: Grattan, J. & Torrence, R. (Ed.) *Living under the shadow: The cultural impacts of volcanic eruptions*. Walnut Creek, USA: One World Archaeology Series. pp. 175–202.

Cronin, S.J., Nemeth, K. & Neall, V.E. (2008) Volcanism and Archaeology. In: Pearsall, D.M. (Ed.) *Encyclopedia of Archaeology*. New York: Academic Press. pp. 2185–2196.

Crosweller, H.S., Arora, B., Brown, S.K., Cottrell, E., Deligne, N.I., Guerrero, N.O. et al. (2012) Global database on large magnitude explosive volcanic eruptions (LaMEVE). *Journal of Applied Volcanology*, 1, 1–13.

Davies, S.M. (2015) Cryptotephras: the revolution in correlation and precision dating. *Journal of Quaternary Science*, 30, 114–130.

Fepuleai, A. (2016) *Establishing a Holocene tephrochronology for Western Samoa and its implication for re-evaluation of volcanic hazards, Geology*. Fiji: University of the South Pacific. p. 352.

Fepuleai, A., Gale, S.J., Wales, N.A., McInerney, S.P.L., Lal, K.K. & Alloway, B.V. (2018) Post-eruptive sedimentary processes in volcanic crater lakes: implications for deciphering the Samoan sedimentary record. *Journal of Paleolimnology*, 60, 473–493.

Firth, C.W., Handley, H.K., Cronin, S.J. & Turner, S.P. (2014) The eruptive history and chemical stratigraphy of a post-caldera, steady-state volcano: Yasur, Vanuatu. *Bulletin of Volcanology*, 76, 837.

Gao, C., Robock, A., Self, S., Witter, J.B., Steffenson, J.P., Clausen, H.B. et al. (2006) The 1452 or 1453 A.D. Kuwae eruption signal derived from multiple ice core records: Greatest volcanic sulfate event of the past 700 years. *Journal of Geophysical Research: Atmospheres*, 111: D15105.

Gosling, W.D., Sear, D.A., Hassall, J.D., Langdon, P.G., Bönnen, M.N.T., Driessen, T.D. et al. (2020) Human occupation and ecosystem change on Upolu (Samoa) during the Holocene. *Journal of Biogeography*, 47, 600–614.

Hart, S.R., Coetzee, M., Workman, R.K., Blusztajn, J., Johnson, K.T.M., Sinton, J.M. et al. (2004) Genesis of the Western Samoa seamount province: age, geochemical fingerprint and tectonics. *Earth and Planetary Science Letters*, 227, 37–56.

Hassall, J.D. 2017. Static or dynamic: reconstructing past movement of the South Pacific Convergence Zone. University of Southampton.

Hawkins, J.W. 1976. Tectonic Setting and Petrology of Samoa-Tonga-Fiji Region.

Hayward, C. (2012) High spatial resolution electron probe microanalysis of tephras and melt inclusions without beam-induced chemical modification. *The Holocene*, 22, 119–125.

Hogg, A.G., Heaton, T.J., Hua, Q., Palmer, J.G., Turney, C.S., Southon, J. et al. (2020) SHCal20 Southern Hemisphere calibration. *0–55,000 years cal BP*, 62, 759–778.

Hopkins, J.L., Bidmead, J.E., Lowe, D.J., Wysoczanski, R.J., Pillans, B.J., Ashworth, L. et al. (2020) TephraNZ: a major and trace element reference dataset for prominent Quaternary rhyolitic tephras in New Zealand and implications for correlation. *Geochronology Discuss*, 2020, 1–63.

Hopkins, J.L., Lowe, D.J. & Horrocks, J.L. (2021) Tephrochronology in Aotearoa New Zealand. *New Zealand Journal of Geology and Geophysics*, 64, 153–200.

Hunt, J.B. & Hill, P.G. (1993) Tephra geochemistry: a discussion of some persistent analytical problems. *The Holocene*, 3, 271–278.

Jochum, K.P., Nohl, U., Herwig, K., Lammel, E., Stoll, B. & Hofmann, A.W. (2005) GeoReM: a new geochemical database for reference materials and isotopic standards. *Geostandards and Geoanalytical Research*, 29, 333–338.

Jochum, K.P. & Willbold, M. (2006) Reference materials in geoanalytical research - Review for 2004 and 2005. *Geostandards and Geoanalytical Research*, 30, 143–156.

Kear, D. (1967) Geological notes on western Samoa. *New Zealand Journal of Geology and Geophysics*, 10, 1446–1451.

Kear, D. & Wood, B.L. (1959) The geology and hydrology of Western Samoa. *New Zealand Geological Survey, Bulletin*.

Kereszturi, G. & Németh, K. (2012). Monogenetic basaltic volcanoes: genetic classification, growth, geomorphology and degradation, Updates in volcanology-new advances in understanding volcanic systems. IntechOpen.

Koppers, A.A.P., Russell, J.A., Jackson, M.G., Konter, J., Staudigel, H. & Hart, S.R. (2008) Samoa reinstated as a primary hotspot trail. *Geology*, 36, 435–438.

Lagomauitumua, F., Seuseu, S.K. & Faasaoina, T. (2011) Chapter 12: Samoa. In: Rischbieth, J. (Ed.) Climate change in the Pacific: Scientific assessment and new research volume 1:. Australian Bureau of Meteorology. Australia: Commonwealth Scientific and Industrial Research Organisation. pp. 185–198.

Latter, J.H., Lloyd, E.F., Smith, I.E.M. & Nathan, S. (1992) *Volcanic hazards in the Kermadec Islands, and at submarine volcanoes between southern Tonga and New Zealand*. Ministry of Civil Defence Volcanic Hazards Information Series 4.

Le Bas, M.J.L., Maitre, R.W.L., Streckeisen, A. & Zanettin, B. (1986) A chemical classification of volcanic rocks based on the Total Alkali-Silica diagram. *Journal of Petrology*, 27, 745–750.

Lowe, D.J. (2011) Tephrochronology and its application: A review. *Quaternary Geochronology*, 6, 107–153.

Lowe, D.J., Blaauw, M., Hogg, A.G. & Newnham, R.M. (2013) Ages of 24 widespread tephras erupted since 30,000 years ago in New Zealand, with re-evaluation of the timing and palaeoclimatic implications of the Lateglacial cool episode recorded at Kaipo bog. *Quaternary Science Reviews*, 74, 170–194.

Lowe, D.J., Shane, P.A.R., Alloway, B.V. & Newnham, R.M. (2008) Fingerprints and age models for widespread New Zealand tephra marker beds erupted since 30,000 years ago: a framework for NZ-INTIMATE. *Quaternary Science Reviews*, 27, 95–126.

Lowe, J.J., Ramsey, C.B., Housley, R.A., Lane, C.S. & Tomlinson, E.L. (2015) The RESET project: constructing a European tephra lattice for refined synchronisation of environmental and archaeological events during the last c. 100 ka. *Quaternary Science Reviews*, 118, 1–17.

Maloney, A.E., Richey, J.N., Nelson, D.B., Hing, S.N., Sear, D.A., Hassall, J.D. et al. (2022) Contrasting Common Era climate and hydrology sensitivities from paired lake sediment dinosterol hydrogen isotope records in the South Pacific Convergence Zone. *Quaternary Science Reviews*, 281, 107421.

Mueller-Dombois, D. & Fosberg, F.R. (1998) Vegetation of the tropical Pacific islands. *Springer Science & Business Media*.

Natland, J.H. (1980) The progression of volcanism in the Samoan linear volcanic chain. *American Journal of Science*, 280, 709–735.

Németh, K. & Cronin, S.J. (2009) Volcanic structures and oral traditions of volcanism of Western Samoa (SW Pacific) and their implications for hazard education. *Journal of Volcanology and Geothermal Research*, 186, 223–237.

Németh, K. & Cronin, S.J. (2011) Drivers of explosivity and elevated hazard in basaltic fissure eruptions: the 1913 eruption of Ambrym Volcano, Vanuatu (SW-Pacific). *Journal of Volcanology and Geothermal Research*, 201, 194–209.

Poli, P. & Shapiro, N.M. (2022) Rapid Characterization of Large Volcanic Eruptions: measuring the Impulse of the Hunga Tonga Ha'apai Explosion From Teleseismic Waves. *Geophysical Research Letters*, 49, e2022GL098123.

Regelous, M., Turner, S., Falloon, T.J., Taylor, P., Gamble, J. & Green, T. (2008) Mantle dynamics and mantle melting beneath Niuafo'ou Island and the northern Lau back-arc basin. *Contributions to Mineralogy and Petrology*, 156, 103–118.

Roman, M., McWethy, D.B., Kehrwald, N.M., Erhenhi, E.O., Myrbo, A.E., Ramirez-Aliaga, J.M. et al. (2021) A multi-decadal geochemical record from Rano Aroi (Easter Island/Rapa Nui): Implications for the environment, climate and humans during the last two millennia. *Quaternary Science Reviews*, 268, 107115.

Sáez, A., Valero-Garcés, B.L., Giralt, S., Moreno, A., Bao, R., Pueyo, J.J. et al. (2009) Glacial to Holocene climate changes in the SE Pacific. The Raraku lake sedimentary record (Easter Island, 27 S). *Quaternary Science Reviews*, 28, 2743–2759.

Shane, P. & Wright, I.C. (2011) Late Quaternary tephra layers around Raoul and Macauley Islands, Kermadec Arc: implications for volcanic sources, explosive volcanism and tephrochronology. *Journal of Quaternary Science*, 26, 422–432.

Smith, V.C., Shane, P. & Nairn, I.A. (2005) Trends in rhyolite geochemistry, mineralogy, and magma storage during the last 50 kyr at Okataina and Taupo volcanic centres, Taupo Volcanic Zone, New Zealand. *Journal of Volcanology and Geothermal Research*, 148, 372–406.

Smith, V.C., Shane, P., Nairn, I.A. & Williams, C.M. (2006) Geochemistry and magmatic properties of eruption episodes from Haroharo linear vent zone, Okataina Volcanic Centre, New Zealand during the last 10 kyr. *Bulletin of Volcanology*, 69, 57–88.

Stearns, H.T. (1944) Geology of the Samoan islands. *Geological Society of America Bulletin*, 55, 1279–1332.

Turner, S., Caulfield, J., Rushmer, T., Turner, M., Cronin, S., Smith, I. et al. (2012) Magma evolution in the primitive, intra-oceanic Tonga arc: rapid petrogenesis of dacites at Fonualei volcano. *Journal of Petrology*, 53, 1231–1253.

Venzke, E. (Ed.). (2013). Global Volcanism Program. v. 4.4.1. ed. Smithsonian Institution, https://doi.org/10.5479/si.GVP.VOTW4-2013.

Wirrmann, D., Eagar, S.H., Harper, M.A., Leroy, É. & Sémah, A.-M. (2011) First insights into mid-Holocene environmental change in central Vanuatu inferred from a terrestrial record from Emaotfer Swamp, Efaté Island. *Quaternary Science Reviews*, 30, 3908–3924.

Witze, A. (2022) Why the Tongan eruption will go down in the history of volcanology. *Nature*, 602, 376–378.

Workman, R.K., Hart, S.R., Jackson, M., Regelous, M., Farley, K.A., Blusztajn, J. et al. (2004) Recycled metasomatized lithosphere as the origin of the Enriched Mantle II (EM2) end-member: evidence from the Samoan Volcanic Chain: Recycled Metasomatized Lithosphere. *Geochemistry, Geophysics, Geosystems*, 5, n/a.

Worthington, T.J., Gregory, M.R. & Bondarenko, V. (1999) The Denham Caldera on Raoul Volcano: dacitic volcanism in the Tonga–Kermadec arc. *Journal of Volcanology and Geothermal Research*, 90, 29–48.

Yeo, I.A., McIntosh, I.M., Bryan, S.E., Tani, K., Dunbabin, M., Metz, D. et al. (2022) The 2019–2020 volcanic eruption of Late'iki (Metis Shoal). *Tonga. Sci Rep-Uk*, 12, 7468.

Zuo, M., Zhou, T., Man, W., Chen, X., Liu, J., Liu, F. et al. (2022) Volcanoes and climate: sizing up the impact of the recent Hunga tonga-Hunga Ha'apai volcanic eruption from a historical perspective. *Advances in Atmospheric Sciences*, 39, 1986–1993.